Conformational Energetics of a Reverse Turn in the *Clostridium beijerinckii* Flavodoxin Is Directly Coupled to the Modulation of Its Oxidation−Reduction Potentials†

Mumtaz Kasim and Richard P. Swenson*

Department of Biochemistry, The Ohio State University, Columbus, Ohio 43210

Received July 5, 2000; Revised Manuscript Received September 18, 2000

ABSTRACT: A surface loop in the flavodoxin from *Clostridium beijerinckii* comprised of residues -Met[56]-Gly-Asp-Glu[59]- forms a four-residue reverse turn which undergoes a conversion from a mix of cis/trans peptide configurations that approximate a type II configuration in the oxidized state to a type II′ turn upon reduction of the bound flavin mononucleotide (FMN) cofactor. This change results in the formation of a new hydrogen bond between the N(5)H of the reduced cofactor and the carbonyl group of Gly57 of the central peptide bond of the turn, an interaction that is thought to contribute to the modulation of the oxidation−reduction potentials of the cofactor [Ludwig, M. L., Pattridge, K. A., Metzger, A. L., Dixon, M. M., Eren, M., Feng, Y., and Swenson, R. P. (1997) *Biochemistry 36*, 1259−1280]. In this study, the direct linkage of the conformational energetics of this turn to the stabilization of the FMN semiquinone was established by systematically replacing the second and third residues of the turn (Gly57 and Asp58) with the -Gly-Gly-, -Gly-Ala-, -Ala-Gly-, and -Ala-Ala- dipeptidyl sequences. On the basis of published position specific preferences for residues with side chains (mimicked by Ala) and glycine, a strong correlation was observed between $E_{ox/sq}$ and the calculated free-energy differences between the type II and type II′ conformations of each of these sequence combinations. The -Ala-Gly- sequence, which favors the type II turn configuration primarily adopted in the oxidized state, displays a $E_{ox/sq}$ value that is about 150 mV more negative than that for the wild-type-like -Gly-Ala- sequence, which prefers the type II′ conformation observed in the reduced states. The -Gly-Gly- and -Ala-Ala- mutants exhibit intermediate $E_{ox/sq}$ values consistent with their ambivalent turn preferences. The potential changes are primarily the result of alterations in the stability of the semiquinone state. These results provide more conclusive evidence for the crucial role of this conformational change in the modulation of the redox potentials of this flavodoxin. Furthermore, this study establishes a direct association between the conformational energetics of the protein, induced in this case by the sequence specificity of a β-turn, and the differential thermodynamic stabilization of specific redox states of the cofactor, demonstrating another means by which flavoproteins can modulate the redox potentials of the bound cofactor.

The structural simplicity and unique redox properties of the flavodoxin, when compared to other flavoproteins, make this a good model system in which to study the protein−flavin interactions responsible for establishing some of the biochemical properties of the cofactor. Furthermore, a flavodoxin-like structural motif has been identified for the FMN-binding[1] domain in a number of other more complex flavoproteins. Flavodoxins are low molecular weight flavoproteins ($\leq$20 kDa) that contain a single noncovalently bound flavin mononucleotide (FMN) as the only redox-active component. They typically thermodynamically stabilize the neutral semiquinone (SQ) state while preferentially destabilizing the anionic hydroquinone (HQ) (*1*, *2*). In this way, the oxidation−reduction potential of the functionally important sq/hq couple is poised at very low values, in some cases approaching −500 mV (pH 7 vs SHE). This contributes to their role as low-potential electron-transfer proteins in a number of essential biological processes such as nitrogen fixation and photosynthesis (*1*, *2*).

A variety of flavin-protein interactions have been shown to play a role in controlling the midpoint potential of the cofactor, including both short and long-range electrostatic interactions (*3*−*6*), aromatic interactions (*3*, *7*, *8*), sulfur-flavin interactions (*9*), and hydrogen-bonding interactions at N(3)H (*10*) and N(5) (*6*, *11*−*13*). Changes in protein-flavin interactions arising from conformational changes also appear to play a crucial role. This phenomenon has been observed for the flavodoxins from *Clostridium beijerinckii* (*11*, *14*, *15*), *Desulfovibrio vulgaris* (*16*, *17*), and *Anacystis nidulans* (*18*, *19*).

† This study was supported in part by Grant GM36490 from the National Institutes of Health.

* To whom correspondence should be addressed. Phone: (614) 292-9428. Fax: (614) 292-6773. E-mail: swenson.1@osu.edu.

[1] Abbreviations: FMN, flavin mononucleotide; OX, oxidized state; SQ, one-electron reduced or semiquinone state, HQ, two-electron reduced or hydroquionone state; ox/sq, oxidized-semiquinone couple; sq/hq, semiquinone-hydroquinone couple; $E_{ox/sq}$ and $E_{sq/hq}$, midpoint potential of the oxidized-semiquinone couple or semiquinone-hydroquinone couple, respectively; HSQC, heteronuclear single-quantum coherence.

10.1021/bi001519a CCC: $19.00
Published on Web 11/18/2000

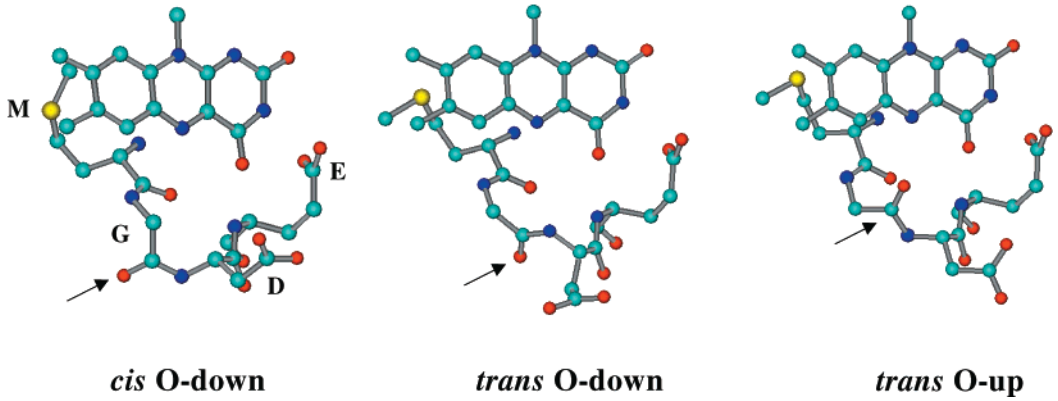

FIGURE 1: Structure of the reverse turn involving residues 56−59 in the *C. beijerinckii* flavodoxin (*11*). The structures "cis O-down" and "trans O-down" represent the predominant conformations of this turn in the oxidized state of the FMN cofactor. The structure "trans O-up" represents the configuration observed in both of the reduced states of the FMN in which the carbonyl oxygen of Gly57 forms a hydrogen bond to the flavin N(5)H. The arrow points toward the carbonyl group at which the rearrangement occurs. The orientation of each figure is slightly different in an effort to optimize the reader's view of the peptide bond between residues 57 and 58. The hydrogen atoms and the ribityl side chain of the FMN have been omitted for clarity.

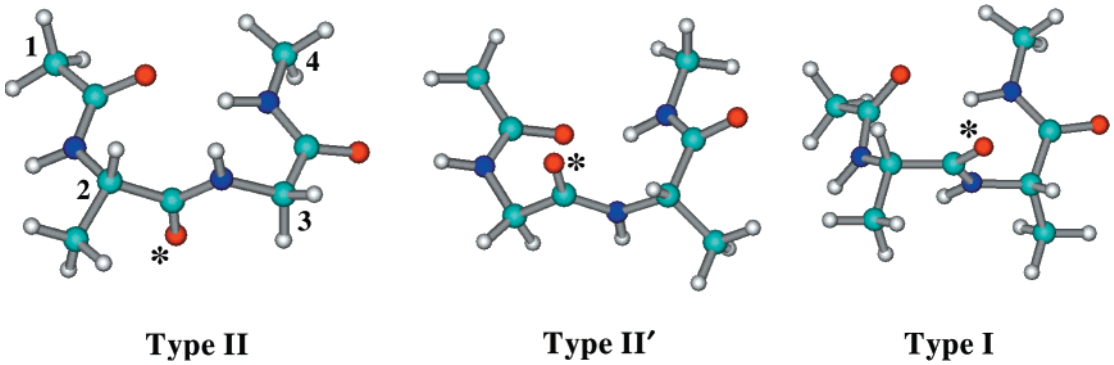

FIGURE 2: Representations of various turn conformations showing the orientation of the central carbonyl group. The residues are numbered near their C_α atom with residues 2 and 3 being the two central residues of the turn. The figure was generated in HyperChem Pro 5.1 using the dipeptide CH_3CO-$X_{(2)}$-$X_{(3)}$-NH-CH_3 with -$X_{(2)}$-$X_{(3)}$- being -Ala-Gly, -Gly-Ala-, or -Ala-Ala- for type II, type II′ and type I turns, respectively, representing the favored sequences for these turn types. The following typical ϕ,ψ angles for these turns were used: for type II $\phi_2 = -60$, $\psi_2 = 120$, $\phi_3 = 90$, and $\psi_3 = 0$ and type I $\phi_2 = -60$, $\psi_2 = -30$, $\phi_3 = -90$, and $\psi_3 = 0$. The ϕ,ψ angles for the type II′ turn are inverse of the type II turn. The orientation of each structure is slightly different in order to optimize the reader's view of the central peptide bond.

For the *C. beijerinckii* flavodoxin, this change occurs in a surface loop comprised of residues -Met[56]-Gly-Asp-Glu[59]-, which forms a reverse turn flanking the C(6)/N(5)/C(4)O edge of the FMN (Figure 1) (for a complete structural description, see ref *11*). In the oxidized state, the peptide bond between Gly57 and Asp58 adopts a mixture of trans and cis configurations that primarily point the carbonyl group away from the flavin ("O-down" configuration). The individual contributions of the various conformers in the oxidized state is estimated to be 50 and 20% for the cis O-down and the trans O-down forms respectively, with the remainder being the trans O-up species. Reduction of the cofactor to the SQ state results in a structural rearrangement involving a rotation or "flipping" of the carbonyl group so that it now points toward the flavin ("O-up" configuration). In this way, the carbonyl group can form a new hydrogen bond with N(5)H of the SQ (*15*) which apparently shifts the equilibrium of the conformers to that favoring the trans O-up species alone. The thermodynamic stabilization of the SQ as a result of hydrogen bond formation contributes significantly to the large separation between the two redox couples and to the relatively high midpoint potential of −92 mV for the ox/sq couple in this protein. No significant structural differences between the SQ and HQ state are apparent (*11*, *15*).

The glycine residue frequently found at the second position of the equivalent turn in several flavodoxins has long been thought to be of functional importance. The conformational change associated with the change in redox state of the FMN approximates the interconversion of a type II reverse- or β-turn (resembling the O-down configuration found in the oxidized state of the flavodoxin) and the type II′ turn (the O-up configuration in the reduced states) (see Figure 2 for the idealized structures of several common β-turn types). Glycine, lacking many of the steric constraints imposed by the presence of a side chain, would appear to favor the formation of the type II′ turn (O-up) configuration, thus contributing to the thermodynamic stabilization of the FMN_{SQ} through the hydrogen-bonding interaction at N(5)H. In fact, the replacement of Gly57 by a series of amino acids in the *C. beijerinckii* flavodoxin results in a more negative midpoint potential for the ox/sq couple (*11*). The crystal structures of the mutants revealed no major structural changes, with all except the G57T adopting in part the unusual cis O-down configuration as in wild-type. Furthermore, all of the mutants are capable of undergoing the O-down to O-up transition upon reduction. This was a particularly surprising observation for the D58P mutant for which this transition represents the cis to trans isomerization of an X-Pro bond, thought to be

separated by a substantial free-energy barrier. These results indicate that most replacements at the two central positions of this turn are accommodated without significantly disrupting the structure and conformational changes associated with the change in the redox state of the FMN cofactor. Yet, the $E_{ox/sq}$ for all the mutants were lower than wild-type. These observations support the view that glycine is favored at the second position in the type II′ turn configuration found in the reduced state and that this preference is critical in the modulation of the redox potentials of this couple (*11*).

A similar conformational change occurs in the *A. nidulans* flavodoxin; however, in this case, the second residue in the turn is an asparagine residue, which based on the above study and sequence preferences should less favorably adopt the type II′ (O-up) conformation in the SQ state. This situation may contribute to the lower $E_{ox/sq}$ of −221 mV in this flavodoxin. In fact, replacement of this asparagine by a glycine resulted in an increase in $E_{ox/sq}$. The proposed increased stability of the type II′ conformation in this mutant appears to be confirmed by the observation that unlike for the wild-type this configuration is retained in the hydroquinone state (*6*, *20*). A series of glycine mutants at the equivalent position (Gly61) in the flavodoxin from *D. vulgaris* was also found to modulate $E_{ox/sq}$ in a manner resembling that of the *C. beijerinckii* flavodoxin, although the structural consequences of this replacement is quite different and may not directly apply to the arguments presented here (*12*, *16*, *17*).

Thus, the evidence so far seems to point to the importance in the flavodoxin of the sequence specificity of the reverse turn near N(5) of the FMN cofactor in the modulation of its reduction potentials, particularly the ox/sq couple. But, how is this specificity translated to the cofactor? Can it be correlated directly to the energetic differences between each turn type? If so, in structural terms, how does this modulate the stability of each redox state of the cofactor? Only recently has a more direct correlation been found between the lower $E_{ox/sq}$ values of the Gly57 mutants of the *C. beijerinckii* flavodoxin and the strength of the hydrogen bond at N(5)H. This was accomplished by measuring the temperature dependency of the chemical shift of the proton on N(5) of the fully reduced FMN by ^{1}H-^{15}N HSQC nuclear magnetic resonance spectroscopy (*13*). The wild-type situation having a glycine residue at position 57 offered the strongest hydrogen bond while substitution with increasingly bulky side chains decreased the hydrogen bond strength in accordance with their size. Although the conformational energetics of this turn was an important determinant of $E_{ox/sq}$, no evidence was sought for the direct role of the stability of the various conformations on these events.

The study presented here was initiated to more systematically investigate the contribution of the position specific preferences for residues with and without side chains at the second and third position of this turn, and to more solidly establish a thermodynamic link between the conformational energetics of this loop and the modulation of the midpoint potential of the FMN cofactor. On the basis of quantitative computational estimates of the energy differences between type II and type II′ turns (*21*, *22*), an attempt was made to correlate the changes in the potentials of the FMN and the conformational energetics of the loop. Alanine was used to represent all residues with side chains with the exception of proline. Using site-directed mutagenesis, the second and third residues of the turn (Gly57 and Asp58) were systematically replaced to -Gly-Ala-, -Gly-Gly-, -Ala-Ala-, and -Ala-Gly- in order to alter the local conformational energies, thus energetically favoring a particular conformation. The results provide conclusive evidence for a direct correlation between $E_{ox/sq}$ and the conformational stability of the turn and underlines the role of this turn in the modulation of redox potentials in this flavodoxin.

EXPERIMENTAL PROCEDURES

Materials. Indigodisulfonate and anthraquinone-2,6-disulfonate were purchased from Fluka Chemicals. Phenosafranin was from Allied Chemical. Benzyl viologen and sodium dithionite were obtained from Aldrich Chemical Co. Flavin mononucleotide was extracted from recombinant wild-type *Clostridium beijerinckii* flavodoxin and purified by anion-exchange chromatography. Sodium 2,2-dimethyl-2-silapentane-5-sulfonate (DSS) and $^{15}NH_4Cl$ (99%) was from Cambridge Isotope Laboratories. All other chemicals were of analytical reagent grade.

Site-Directed Mutagenesis and Protein Expression and Purification. The synthetic gene for the flavodoxin from *C. beijerinckii* has previously been prepared and cloned into the phagemid p*Bluescript* (p*BSFlasy*). Mutagenesis was carried out using the Kunkel method (*23*). Three mutagenic oligonucleotides that were synthesized for the generation of the different Gly/Ala dipeptidyl sequence combinations at positions 57 and 58 in the flavodoxin were as follows: 5′GCCATGGGCGMTGMAGT(A)CTCGAGG for -Gly-Ala-; 5′GCTCTGCCATGGCCGCGGAAGTTCTCG for -Ala-Ala-; 5′GCTCTGCCATGGSCGGCGAAGT(A)CTCG for -Gly-Gly- and -Ala-Gly- (where M = A and C and S = G and C). The nucleotide in parentheses is a silent mutation that introduces a unique restriction site (*Sca*I) for screening purposes. The underlined positions are the altered sites that introduce the appropriate amino acid replacement. The degenerate oligonucleotide creating the -Gly-Ala- sequence was designed to also produce the E59A and D58A/E59A mutants for other studies. Mutagenesis generating the -Gly-Ala- sequence introduces a unique *Hae*II site; a *Sst*II site for the -Ala-Ala- sequence; and a *Nae*I site for -Ala-Gly- that was absent in the -Gly-Gly- mutant. In this way, all of the mutants were initially screened and identified by restriction mapping; however, all mutations and the sequence integrity of the entire flavodoxin gene, including within the following expression constructions, were confirmed by automated DNA sequence analysis. All mutants were subcloned into the *Eco*RI and *Hin*dIII sites of the pKK223-3 expression vector for heterologous expression in the XL-1 Blue strain of *Escherichia coli*. Protein purification was carried out by established protocols (*3*). Expression levels for all mutant proteins were comparable to wild-type flavodoxin. All proteins were >95% pure as determined by SDS−PAGE.

UV−Vis Spectroscopy and Determination of One-Electron Oxidation−Reduction Potentials. All UV−vis spectra were recorded on a Hewlett-Packard HP8452A diode array spectrophotometer. The one-electron oxidation−reduction potentials were determined as described elsewhere (*3*, *4*). All measurements were performed at 25 °C in 50 mM sodium phosphate buffer, pH 7.0. The indicator dyes used were

indigodisulfonate (−116 mV), anthraquinone-2,6-disulfonate (−184 mV), phenosafranin (−244 mV), and benzyl viologen (−359 mV). The midpoint potentials for the dyes indicated in parentheses are at 25 °C, pH 7.0 versus the standard hydrogen electrode (*24*). The estimated error of the experimental values reported here is within ± 5 mV.

Fluorescence Spectroscopy and Determination of FMN Dissociation Constants in the Oxidized State. Flavin fluorescence was measured on a Perkin-Elmer LS50B spectrophotometer. Fluorescence emission was recorded at 522 nm with excitation at 445 nm after allowing sufficient time for equilibration. Experimental conditions were the same as for the oxidation−reduction potential determinations. The concentration of the FMN solutions was determined using the published extinction coefficient of 12 500 M^{-1} cm^{-1} (*25*). Apoflavodoxin was prepared as previously described by the trichloroacetic acid precipitation technique (*26*). The K_d for oxidized FMN was determined by nonlinear regression analysis of the fluorescence emission plotted as a function of added apoflavodoxin (*9*). The dissociation constants for the SQ and HQ states, which cannot be determined directly, were calculated using a thermodynamic cycle linking the K_d for oxidized FMN and the one-electron reduction potentials for the various redox states for both the bound and free FMN. The one-electron reduction potentials for free FMN used in this study were those determined by Anderson (*27*), which have recently been reported (*28*) to be more reliable than those of Draper and Ingraham (*29*) previously used.

Preparation of ^{15}N-Enriched FMN, Reconstitution with Apoflavodoxin and One- and Two-Dimensional NMR Spectroscopy. FMN uniformly enriched at all four nitrogen atoms with >95% ^{15}N was prepared and used to reconstitute apoflavodoxin according to the procedure detailed by Chang et al. (*13*). 1D-NMR spectra were recorded for approximately 2 mM solutions of the oxidized flavodoxin samples in 50 mM phosphate buffer, pH 7, containing 10% D_2O as described previously (*13*). These samples were also used for the ^{1}H-^{15}N HSQC experiments, but were first reduced by the addition of freshly prepared sodium dithionite under anaerobic conditions. Proton chemical shifts were referenced to an internal standard of sodium 2,2-dimethyl-2-silapentane-5-sulfonate (DSS) set at 0.0 ppm. The details of the method have been described elsewhere (*13*).

RESULTS

UV−Vis Spectral Characteristics of the Mutant Flavodoxins. Four mutants of the *C. beijerinckii* flavodoxin were generated with all possible dipeptidyl sequence combinations containing glycine and alanine residues at positions 57 and 58, the central residues within the targeted reverse turn in this protein. All proteins were heterologously expressed in *E. coli* at high yields comparable to wild-type. The purified holoproteins all exhibited a A_{274}/A_{446} ratio of 4.4 ± 0.1, a value similar to wild-type and characteristic of a 1:1 cofactor−protein complex. The spectral characteristics of all three redox states were recorded during a reductive titration with sodium dithionite under anaerobic conditions for each mutant. The visible absorbance spectrum for the -Gly-Ala- mutant in the oxidized state is very similar to the wild-type flavodoxin (Figure 3, solid line). The -Gly-Gly-, -Ala-Ala-, and -Ala-Gly- mutants display very similar spectral properties as a group, displaying small spectral shifts in the 450 nm region compared to wild-type and the -Gly-Ala- mutant (see Figure 3). The extinction coefficients for the 450 nm transition were determined to be within experimental error about the same for all the holoproteins. It is difficult to interpret these small spectral changes with certainty because many factors are influential. They could be the result of a slight increase in solvent exposure of the flavin ring or slight changes in the flavin−protein interactions (*30*).

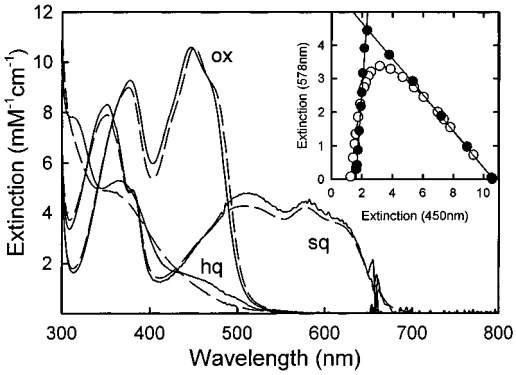

FIGURE 3: UV−vis absorbance spectra for the *C. beijerinckii* -Gly-Ala- (solid lines) and the -Ala-Gly- (dashed lines) flavodoxin mutants in all three oxidation states obtained during a reductive titration with sodium dithionite in 50 mM sodium phosphate buffer, pH 7.0 at 25 °C. The inset shows a plot of the absorbance changes at 450 nm (primarily due to the oxidized FMN) versus 580 nm (flavin semiquinone) during the course of the titration for the -Gly-Ala- mutant (closed circles) and the -Ala-Gly- mutant (open circles).

The neutral form of the FMN semiquinone accumulates in all the mutants during the anaerobic reduction with dithionite. Except for the -Ala-Gly- protein, the SQ is generated in direct proportion to the loss of the oxidized state until it was completely consumed. Results shown for the -Gly-Ala- in the inset in Figure 3 (closed circles) are representative. Note the linearity of the absorbance changes at 578 nm due to the SQ versus those at 450 nm primarily due to the oxidized state. The second step also proceeds with the proportional conversion of the SQ to the HQ. The two redox couples are obviously well-separated in these proteins. For the -Ala-Gly- mutant, however, the HQ began to form before all of the oxidized species has been reduced to the SQ (Figure 3, inset, open circles). In all cases, the spectral characteristics of the semiquinone are similar to wild-type, with no obvious trends in the difference spectra. On the other hand, distinct spectral differences for the FMN hydroquinone are noted among this group of proteins. Two peaks at 315 and 367 nm and a shoulder at 450 nm characterize the wild-type hydroquinone spectrum. The -Gly-Ala- and -Gly-Gly mutants are the most similar to the wild-type spectrum, displaying spectral perturbations that can be generally characterized as a slight decrease in extinction for all three transitions. The spectral characteristics of the -Ala-Ala- and -Ala-Gly- mutants are comparable and the most perturbed, lacking the distinguishing features of the wild-type. Most notable is the marked reduction in the shoulders at 367 and 450 nm, particularly for the -Ala-Ala- mutant. Although the differences are small, it is perhaps of interest that the spectral perturbations for the HQ seem to segregate with the presence of either a glycine or an alanine at position 57. On the basis of model compounds, the spectral features of the wild-type

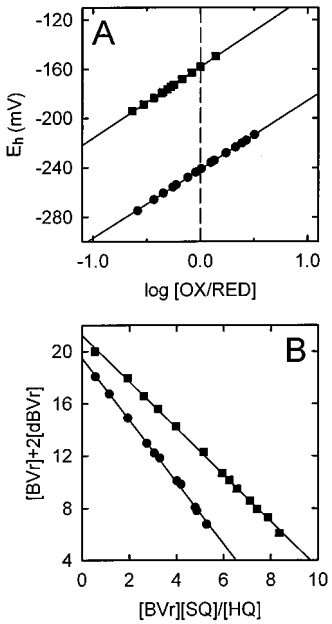

FIGURE 4: Representative determinations of $E_{ox/sq}$ (A) and $E_{sq/hq}$ (B) for the -Ala-Gly- (closed circles) and the -Ala-Ala- (closed squares) mutants. The data in panel A are plotted according to the linear version of the Nernst equation using the system potential (E_h) as determined by the concentration of the oxidized and reduced forms of the redox indicator dye in equilibrium with the flavodoxin during the titration. The $E_{sq/hq}$ values were calculated from the equilibrium concentrations of the semiquinone and hydroquinone forms of each flavodoxin mutant together with the monomeric (BVr) and dimeric (dBVr) forms of reduced benzyl viologen during each step of a reductive titration as documented previously (*4*).

flavodoxin have been suggested as representing the planar, anionic form of the flavin (*31*); however, it is possible that the spectrum of the hydroquinone is sensitive to other changes in its environment (*32*).

One-Electron Oxidation−Reduction Potentials. The one-electron oxidation−reduction potentials of the mutants were determined at 25 °C in 50 mM sodium phosphate buffer, pH 7.0, during reduction with sodium dithionite under anaerobic conditions in the presence of an indicator dye with an established midpoint potential (*24*). The titration data sets for this group of proteins could be fit to the linear version of the Nernst equation with a slope of 59 ± 5, indicative of a transfer of a single electron accompanied by the uptake of a proton generating the observed neutral form of the semiquinone. Representative Nernst plots for the redox titrations for the -Ala-Gly- and -Ala-Ala- mutants are shown in Figure 4A. It is quite apparent that the midpoint potential of the FMN cofactor is very sensitive to the dipeptidyl sequence of the two central residues in the turn, particularly for the ox/sq couple. With the exception of the -Gly-Ala- mutant, which displays an $E_{ox/sq}$ value very similar to wild-type, the midpoint potentials for these proteins were substantially more negative than for wild-type (Table 1). Both the -Gly-Gly- and -Ala-Ala- mutants had similar potential values of −157 and −158 mV, respectively. The -Ala-Gly- mutant exhibited a significantly more negative value of −241 mV. This represents a rather remarkable decrease of nearly 150 mV relative to wild-type and the -Gly-Ala- mutant, given that this difference is, in its simplest terms, the consequence of the movement of a single methyl group by one amino acid position within this protein! The midpoint potentials for the sq/hq couple were determined by equilibration with benzyl viologen as the indicator dye by methods described previously (*4*). Representative plots of such a titration is shown in Figure 4B for the -Ala-Gly- and -Ala-Ala- mutants. All mutants exhibited $E_{sq/hq}$ values that were less negative than wild-type (Table 1); however, the changes are much less pronounced than for the ox/sq couple. The increase of 19 mV for the -Gly-Ala- mutant is identical to that observed for the D58S mutant previously characterized (*11*) and is consistent with the loss of the electrostatic effect associated with the removal of a single negatively charged residue near the FMN (*4*).

It is essential for the interpretation of the results of this study to establish that endogenous side-chain interactions in the wild-type protein by themselves would not affect the potentials, particularly for the ox/sq couple. The only relevant residue in this case is Asp58 as a glycine is normally found at position 57. For this, the -Gly-Ala- mutant serves as a good control. The $E_{ox/sq}$ for this mutant (−93 mV) does not differ from wild-type (-Gly-Asp-) (−92 mV). Furthermore, the previously characterized D58S mutant (i.e., -Gly-Ser-) has an $E_{ox/sq}$ value of −89 mV (*11*). Similarly, the $E_{ox/sq}$ for the -Ala-Ala- mutant (−158 mV) is comparable to that for the G57A mutant (i.e., -Ala-Asp-) (−143 mV) previously characterized (*11*). Thus, these examples serve to establish that it is not the physicochemical nature of the particular side chain that is important in establishing the potential changes observed in the group of mutants reported here but rather the local effects of the various combinations of glycine and alanine on the conformational energetics of the turn as will be argued in depth later. Also of significance, these data indicate that an alanine residue can be representative of nonprolyl residues with side chains in establishing the potentials of this couple. This assumption is also crucial in the computational studies evaluating the energetics of reverse turns (*21*, *22*). Direct evidence to validate the above assumption comes from the free-energy landscapes of these various dipeptides in water that were computed by the enhanced conformational sampling method (*33*). The free-energy landscapes of the -Gly-Ser- and -Gly-Ala- dipeptides were identical, as were those of the -Asn-Gly- and -Ala-Gly- dipeptides, conclusively proving that the identity of a particular amino acid side chain has little to do with the overall free energy of the peptide.

The Dissociation Constants and Binding Free Energy Changes for the FMN. The dissociation constants were measured in the oxidized state, making use of the quenching of the FMN fluorescence upon binding to the apoprotein. A representative plot of the fluorescence changes as a function of added apoprotein for the -Ala-Gly- and -Ala-Ala- mutants is shown in Figure 5. The K_d values in each case were obtained from the fit of these data to a binding isotherm involving a 1:1 complex as described in the Experimental Procedures. With the exception of the -Ala-Ala- mutant, which increased about 10-fold, the mutants bound FMN in the oxidized state with values comparable to wild-type (Table 1). The tight binding observed for most of the mutants is consistent with the absence of significant perturbations in flavin-protein contacts in the oxidized state.

The dissociation constants for the FMN cofactor in its two reduced states cannot be established directly due to their instability in solution. However, because the free-energy

Table 1: Oxidation-Reduction Midpoint Potentials,[a] FMN Dissociation Constants,[b] and Gibbs Free Energy[c] Changes of Wild-Type and Mutant *C. beijerinckii* Flavodoxins

			K_d					
flavodoxin	$E_{ox/sq}$ (mV)	$E_{sq/hq}$ (mV)	OX (μM)	SQ (nM)	HQ (μM)	ΔG^{OX}	ΔG^{SQ}	ΔG^{HQ}
wt[d]	−92	−399	0.018	0.0032	0.14	−10.6	−15.7	−9.3
-Gly-Ala-	−93[e]	−380[h]	0.042 ± 0.02	0.0077	0.16	−10.1	−15.2	−9.3
-Gly-Gly-	−157[f]	−367[h]	0.021 ± 0.009	0.046	0.60	−10.5	−14.1	−8.5
-Ala-Ala-	−158[f]	−345[h]	0.15 ± 0.01	0.34	1.9	−9.3	−12.9	−7.8
-Ala-Gly-	−241[g]	−337[h]	0.015 ± 0.005	0.87	3.5	−10.7	−12.4	−7.4

[a] Values are in millivolts at pH 7.0 and 25 °C. [b] The dissociation constants in the oxidized state were measured by fluorescence spectroscopy and those for the reduced states calculated as described in the Experimental Procedures. Values are an average of two independent titrations each done in duplicate. [c] Values are in kilocalories per mole. [d] From Ludwig et al. (*11*) and Druhan et al. (*9*). [e] Midpoint potential was determined using indigo disulfonate as the indicator dye. [f] Midpoint potential was determined using anthraquinone-2,6-disulfonate as the indicator dye. [g] Midpoint potential was determined using phenosafranin as the indicator dye. [h] Midpoint potential was determined using benzyl viologen as the indicator dye. All midpoint potential values are an average of at least two independent titrations.

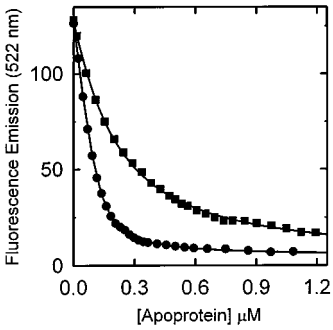

FIGURE 5: Representative binding titrations for the determination of the dissociation constant of the FMN cofactor in the oxidized state are shown for the -Ala-Gly- (circles) and -Ala-Ala- (squares) mutants. In each case, a FMN solution (~0.1 μM) in 50 mM sodium phosphate buffer, pH 7.0 at 25 °C was titrated with increasing amounts of a 50−60 μM apoprotein solution having an identical buffer composition. Data were corrected for dilution. The solid lines represent the best nonlinear regression fit of the data to a binding isotherm for a 1:1 complex, also from which the dissociation constants was derived.

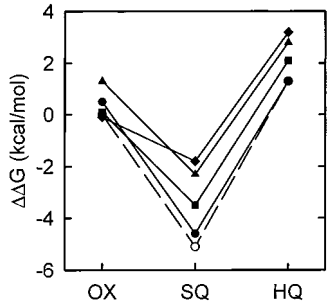

FIGURE 6: Diagram depicting the free energy of binding of the FMN cofactor in all three oxidation states to wild-type (open circles) and mutant *C. beijerinckii* flavodoxins: -Gly-Ala- (closed circles), -Gly-Gly- (squares), -Ala-Ala- (triangles), and -Ala-Gly- (diamonds). All values are relative to the binding free energy for the oxidized cofactor to wild-type flavodoxin.

changes associated with binding or a change in redox state are pathway independent, these values can be calculated using the midpoint potentials for free and bound FMN together with the K_d for oxidized FMN via the appropriate thermodynamic cycle (*34*). With the exception of the -Gly-Ala- mutant, this group of mutants formed significantly weaker complexes with both reduced states of the FMN than as observed for wild-type. The -Ala-Gly- mutant displays a K_d value for the FMN_{SQ} that is about 100-fold higher than for the -Gly-Ala- sequence despite the identity of the amino acids involved. The K_d for the FMN_{SQ} for the -Ala-Ala- mutant was increased 45-fold compared to the oxidized state, which had increased by only 4-fold. Despite these increases, it is clear that the SQ is still the most thermodynamically favorable oxidation state just as for wild-type. Alterations in the dissociation constants for the FMN_{HQ} followed a trend similar to that observed for the FMN_{SQ}; however, the relative increase is an order of magnitude less than for the FMN_{SQ}.

The effects of these mutations can be better visualized when one compares the changes in the free energy of binding of the FMN cofactor in each of the three redox states (Figure 6 and Table 1). With exception of the -Ala-Ala- mutant, all display binding free-energy values that are within 0.5 kcal/mol of wild-type in the oxidized state. The SQ and HQ complexes are all substantially less stable than wild-type except for the -Gly-Ala- mutant, which more closely resembles wild-type in all three oxidation states. As indicated earlier, the -Gly-Ala- mutant will be used for comparison instead of wild-type in order to avoid electrostatic contributions from the aspartate side chain, which has been uniformly removed in all cases, although either comparison generates qualitatively similar conclusions. The -Ala-Gly- mutant displays the largest changes in the free energy of binding in the reduced states. The SQ complex has been destabilized by about 2.8 kcal/mol and the HQ complex by about 1.8 kcal/mol. These increases fall to more intermediate corresponding values of about 1.1 and 0.8 kcal/mol for the -Gly-Gly- mutant. The -Ala-Ala- mutant exhibits increases for the SQ and HQ complexes that are similar to the -Ala-Gly- mutant; however, these changes must be viewed in the context of the significantly less stable complex in the initial oxidized state. If one normalizes or corrects for this initial instability (by assuming that the interaction responsible uniformly affects all three redox states), then the relative increase in the free energy of binding is similar to the -Gly-Gly- mutant, lying intermediate between the -Gly-Ala- (and wild-type) and -Ala-Gly- proteins. Despite this, it is quite obvious that the stability of the SQ complex is principally affected by these alterations in the loop sequence. It will be argued below that the destabilization of the reduced states is likely to be the result of differences in conformational free energy between the type II configuration of the turn in the oxidized state and the type II′ conformer in the reduced state which primarily affects the stability of the SQ complex.

^{15}N- and ^{1}H−Nuclear Magnetic Resonance Spectroscopy. The effects of the various Gly/Ala combinations on the interactions between the protein and the cofactor were

Table 2: ^{15}N Chemical Shifts for Free and Bound FMN in the Oxidized State at pH 7.0, 300 K

	^{15}N chemical shifts (ppm)							
atom	FMN[a]	TARF[a]	CMP[a]	rCB[b]	-Gly-Ala-	-Gly-Gly-	-Ala-Ala-	-Ala-Gly-
N(1)	190.8	199.9	184.5	183.7	182.9	184.2	184.3	184.1
N(3)	160.5	159.8	161.1	160.3	159.1	159.1	158.9	158.9
N(5)	334.7	344.3	351.5	350.9	348.5	341.9	341.7	341.2
N(10)	164.6	150.2	164.8	163.9	162.3	161.5	161.4	161.2

[a] From Vervoort et al. (*36*). [b] From Chang et al. (*13*). Abbreviations: TARF, tetraacetyl-riboflavin in $CHCl_3$; CMP, *Clostridium MP (beijerinckii)* flavodoxin; rCB, recombinant *Clostridium beijerinckii* flavodoxin.

evaluated by ^{15}N- and ^{15}N-^{1}H HSQC-nuclear magnetic resonance spectroscopic analyses of the flavodoxins reconstituted with uniformly ^{15}N-enriched FMN. Emphasis was placed on the evaluation of the effects of the amino acid replacements on hydrogen-bonding interactions at N(1), N(3), and N(5), particularly in the oxidized state. The N(1) and N(5) atoms in the oxidized flavin represent the pyridine-like or β-type nitrogen atoms. The chemical shifts of such atoms are quite sensitive to hydrogen bonding, displaying large upfield shifts. Both N(3) and N(10) in oxidized FMN as well as all four nitrogen atoms in the reduced state are pyrrole-like or α-type nitrogen atoms. The chemical shifts of such atoms show only small downfield shifts on hydrogen bonding (*35*). For comparison, the ^{15}N chemical shift values for unbound FMN and the wild-type *C. beijerinckii* flavodoxin were taken from Vervoort et al. (*36*) and Chang et al. (*13*).

The N(5) chemical shift of the -Gly-Ala- mutant is slightly upfield of wild-type but remains significantly downfield from TARF in chloroform for which hydrogen bonding is not possible. This suggests that the N(5) atom is not hydrogen bonded and is in a relatively apolar environment in the oxidized state for this mutant (Table 2). All the other mutants displayed chemical shifts for N(5) that were significantly upfield relative to the -Gly-Ala- mutant. However, even though the chemical shifts were slightly more upfield than for TARF in chloroform, they remained significantly downfield relative to FMN in aqueous solutions, suggesting that these upfield shifts are unlikely to be the result of strong hydrogen-bonding interactions with solvent. As the apoprotein is incapable of forming a hydrogen bond with N(5) of the flavin in the oxidized state, the upfield shifts are more likely a result of changes in the local environment and/or to differences in the conformer equilibrium of the loop in this group of mutants (*13*). The N(1) chemical shifts of the mutants are all similar to wild-type, being upfield of that of FMN in aqueous solution, conforming to the previous observation of a strong hydrogen bond at this position in this flavodoxin (*36*).

The N(3) chemical shifts of the mutants are similar and upfield of that of the isoalloxazine ring in polar and apolar solutions. It is likely that the N(3) hydrogen-bonding interaction is similar to wild-type in all of these mutants, a conclusion that is supported by strong correlation peaks for the N(3)H in the ^{15}N-^{1}H HSQC NMR spectra in the oxidized state that exhibit temperature coefficients that are comparable to wild-type (data not shown). Because the N(10) atom cannot form hydrogen bonds, the slight upfield shift for this atom in all mutants is probably due to a decrease in sp^2 hybridization as a result of the decrease in polarization of the isoalloxazine ring caused by a weakened hydrogen bond with C(4)O and/or C(2)O (*36*). As these mutations are located near the N(5)/C(4)O flavin edge, a weakened interaction with C(4)O is conceivable. Changes in the chemical shift for N(5) in the mutants are in agreement with the NMR data obtained for several glycine 57 mutants previously prepared and characterized (*13*). Unfortunately, ^{15}N-^{1}H HSQC signals were not observed for either the N(3)H and N(5)H in the reduced state for all the mutants at the field strengths provided by either 600 or 800 MHz spectrometers. The absence of either signal as has been noted in several other flavodoxin mutants and may be the consequence of local conformational dynamics affecting the T_2 relaxation rate or possible the solvent exchange rates (unpublished results). Had these experiments been feasible, the temperature dependency of the chemical shift of particularly the N(5)H would have provided a measure of any alterations in the hydrogen-bonding strength in this group of mutants, data which significantly strengthened the overall conclusions for other Gly57 mutants (*13*).

DISCUSSION

The conformational change associated with the reduction of the FMN cofactor in the *C. beijerinckii* flavodoxin can be adequately described as the conversion of predominantly a type II reverse- or β-turn, albeit in a mix of cis and trans configurations for the central peptide bond, in the oxidized state to that of a type II′ turn in the reduced states (see Figures 1 and 2). This change appears to be facilitated by the presence of a glycine residue at the second position of the turn (*11*) as residues other than glycine rarely populate that position in type II′ turns (*37*, *38*). Glycine lacks the Cβ atom that would otherwise be involved in steric clashes with the NH of the adjacent residue (*39*). Furthermore, type II′ turns require the second residue to adopt positive ϕ values for which glycine and asparagine have the highest propensities. It is not surprising then that the residue that replaces this glycine in many long-chain flavodoxins is an asparagine (*2*). Questions are raised as to whether the relative sequence-derived stability of type II versus type II′ turns has a role in this conformational change and whether the conformational energetics associated with this transition are directly linked to the modulation of the redox potentials of the FMN cofactor.

Several computational studies have attempted to quantify the conformational energetics associated with the sequence specificity of various reverse turns. Their results prompted a possible means to gain greater insight into these questions. Using either a molecular dynamics simulation approach or a Monte Carlo sampling technique as well as molecular mechanical force fields in combination with a solvation model, Yan et al. (*21*) and Yang et al. (*22*) independently calculated the free-energy differences between various types

of β-turn conformers for a series of blocked dipeptides representing the central residues in such turns. Because the conformational energies are thought to be primarily a function of local interactions with the backbone atoms and to simplify the calculations, alanine was used to represent all nonprolyl amino acid residues having side chains and, of course, glycine without. Sequence preferences for a particular turn type were found to be a direct result of the intrinsic conformational preferences of the different residues occupying each of the specific central positions of the turn.

On the basis of their calculations, Yan et al. obtained free-energy differences between the type II′ and type II turn for the sequences -Gly-Ala-, -Ala-Ala-, and -Ala-Gly- of −1.82, 1.01, and 2.83 kcal/mol, respectively. The corresponding values derived by Yang et al. are −4.0 kcal/mol, −2.0 and 1.5 kcal/mol. The free-energy difference for the -Gly-Gly- sequence is negligible due to its symmetry. The inconsistencies in results among various computational studies have recently been shown to be the direct result of the different force fields used (*33*). However, it is the relative differences in the conformational free energies among the sequences that are of concern in our evaluations, and irrespective of the parameters used, the same conclusions are reached. From these data, one can unambiguously conclude that the -Gly-Ala- sequence strongly favors the type II′ turn while the -Ala-Gly- sequence prefers the type II turn, the energy difference between both situations being >4.5 kcal/mol. The calculated relative stability of each of the β-turn conformers is also consistent with their frequency of occurrence in the crystal structures of native proteins (*21*, *22*, *33*). The stability of the -Ala-Ala- sequence relative to the -Gly-Gly- sequence is somewhat ambiguous, preferring a type II′ configuration in the Yang et al. analysis and showing a slight preference for the type II turn in the Yan et al. study. Furthermore, the -Ala-Ala- dipeptidyl sequence may actually have a greater preference for the type I turn configuration (see Figure 2) (*22*, *33*, *40*). As will be addressed further below, these ambiguities do not substantially affect the conclusions of our study, however.

Midpoint Potentials for the Flavodoxin Correlate with Conformational Free-Energy Differences of the Turn. Within the context of these computational studies, the experimentally derived midpoint potential values for both flavin couples for the group of flavodoxin mutants studied here were observed to correlate remarkably well with both sets of the calculated conformational free-energy differences between type II′ and type II turns (Figure 7). It is quite evident that the -Gly-Ala- sequence, which favors the type II′ turn, like the wild-type flavodoxin, has the least negative $E_{ox/sq}$ value, while the -Ala-Gly- sequence, which substantially favors the type II turn, displays the most negative reduction potential. The decrease in $E_{ox/sq}$ for the -Ala-Gly- mutant by nearly 150 mV is a particularly extraordinary consequence of what on the face of it represents a "simplistic" reversal of the Gly/Ala positioning in this turn (i.e., -Gly-Ala- versus -Ala-Gly-). It is difficult to interpret this phenomenon in any other way than as an effect on the conformational energetics/dynamics of the turn in relation to the conformational changes associated with the reduction of the FMN cofactor. On the basis of the crystal structures of the various redox states of this flavodoxin, the tendency for a particular dipeptidyl sequence to prefer a type II turn should favor the oxidized state, making reduction more difficult, while conversely the type II′ turn should favor the reduced states. Accordingly, the -Gly-Gly- and -Ala-Ala- mutants, containing dipeptidyl sequences that exhibit only relatively small free-energy differences between the two turn types, should have potential values that would lie between these two extremes. It is quite apparent that the experimental results are completely consistent with these preferences.

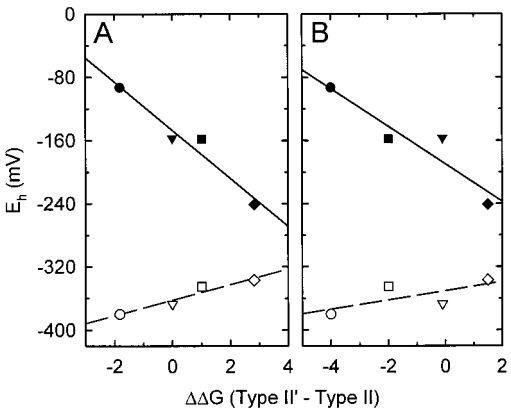

FIGURE 7: Correlation between the midpoint potential values (in mV, pH 7) for the ox/sq couple (closed symbols) and for the sq/hq couple (open symbols) and the calculated conformational free-energy differences between type II′ and type II turns (in kcal/mol) obtained from Yan et al. (A) (*21*) and Yang et al. (B) (*22*). The absolute free-energy differences reported by these two groups differ for reasons given in the Discussion; however, the relative differences between turn types are comparable. Both energy sets are plotted here for comparison and their differences do not affect the overall conclusions of this study. Symbols are as follows: -Gly-Ala-, circles; -Gly-Gly-, *inverted triangles*; -Ala-Ala-, squares; and -Ala-Gly-, diamonds.

The similarity in the $E_{ox/sq}$ values for the -Gly-Gly- and -Ala-Ala- mutants was not predicted from the computational studies. It is possible that the loop in the -Ala-Ala- mutant alternatively adopts a type I turn as is preferred for alanine-containing turns (*22*, *33*, *40*). However, the molecular modeling of a type I turn into the loop suggests that this configuration is poorly accommodated and geometry optimization calculations using the AMBER molecular mechanical force field resulted in the turn reverting to conformational parameters more like that of a type II′ turn (results not shown). In fact, the loop structure of the reduced G57D mutant previously characterized (which is equivalent to the Ala-Ala mutant in terms of the presence of a side chain at both positions), while similar to wild-type, displays slight differences in the torsion angles at positions 56 and 57 to reduce the overlap of the β-carbon with the amide NH of residue 58, a major unfavorable feature of the type II′ turn (*11*). This suboptimal situation may be reflected in the higher K_d for the oxidized FMN in the -Ala-Ala- mutant. In either configuration, a conformational change would not be required to form the hydrogen bond at N(5)H; therefore, one might predict that there would not be a free-energy difference between the oxidized and reduced states as should also be the case for the -Gly-Gly- sequence.

Conformational Energetics of the Reverse Turn Is Coupled to the Modulation of the Oxidation−Reduction Potentials of the FMN Cofactor. The data persuasively associate a significant role of the conformational energetics of the reverse turn to the regulation of the midpoint potentials of

Scheme 1: Thermodynamic Cycles Describing the Free Energies Associated with the Conformational Changes and FMN Binding in Each Oxidation State[a]

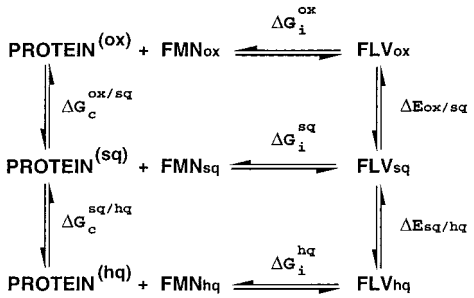

[a] PROTEIN(ox, sq, hq) represents "virtual" forms of the apoflavodoxin having the same structure as the holoflavodoxin (FLV) in each oxidation state but without the bound cofactor. These forms are incorporated in the scheme in order to separate the free energies associated with the conformational changes (ΔG_c) from those associated with the direct protein-flavin interactions (ΔG_i). See also refs *1* and *10*.

the flavin cofactor in this flavoprotein. But, how are the changes in the protein conformational energy translated to the modulation of the flavin potentials? A thermodynamic scheme has been proposed previously that separates energy changes that result from protein conformational changes (ΔG_c) from changes in FMN−protein interactions (ΔG_i) (Scheme 1) (*9*, *11*). The reverse turn in question can be considered to exist in an equilibrium between the O-down (resembling a type II turn) and the O-up (type II′ turn) conformers, with the two states separated by the free-energy change ΔG_c (depending on the couple involved, this change is designated $\Delta G_c^{ox/sq}$ or $\Delta G_c^{sq/hq}$ in Scheme 1). The formation of a new N(5)H···O(57) interaction contributes to the stability of the reduced states by the free-energy difference ΔG_i. The midpoint potential of the bound FMN is a function of the free-energy difference between the two oxidation states concerned. For the ox/sq couple, the free-energy difference would be equal to $\Delta G_c^{ox/sq} + (\Delta G_i^{sq} - \Delta G_i^{ox})$. The amino acid substitutions could either affect the protein conformational energy directly or affect the energy of the FMN-protein interaction or some combination of the two.

Can the observed changes in binding free energy be accounted for by the conformational energetics alone? A difference of approximately 3.4 kcal/mol was noted between the -Gly-Ala- and -Ala-Gly- mutants in the change in the binding free energy in going from the OX to the SQ states of the FMN [i.e., from Table 1; $[\Delta G^{SQ}_{(-Ala-Gly-)} - \Delta G^{OX}_{(-Ala-Gly-)}] - [\Delta G^{SQ}_{(-Gly-Ala-)} - \Delta G^{OX}_{(-Gly-Ala-)}] = [-12.4 - (-10.7)] - [-15.2 - (-10.1)] = 3.4$ kcal/mol]. This value represents about 75% of the free-energy difference between the two turn types, i.e., ΔΔG (II′-II) in Figure 7. Therefore, it is quite possible to account for all of the observed free-energy changes by the effects of the sequence changes on ΔG_c if one reasonably assigns $\Delta\Delta G$ (II′ − II) as the primary component of the ΔG_c term. However, do the amino acid substitutions have any effect on the strength of the N(5)H···O(57) interaction itself, i.e., ΔG_i? This is a difficult question to answer. It is not possible to adequately separate experimentally the ΔG_c and ΔG_i terms. Only small changes in the geometry and interatomic distances were noted for most of the G57 mutants previously characterized, suggesting that the hydrogen-bonding interaction, which contributes to ΔG_i, should remain substantially unaltered (*11*). However, a link between amino acid replacements in this region and changes in the interactions at N(5)H has been established through the determination of the temperature dependency of the chemical shift for the N(5)H of the FMN_{HQ}, which serves as an indicator of the relative strength of the hydrogen bond (*13*). Thus, it is quite likely that a similar situation occurs with these substitutions. Unfortunately, an HSQC NMR signal for the N(5)H in the reduced state was not detected for any of the mutants, an unexpected observation but one also noted previously for the D58P mutant (*13*). Interestingly, based on these and other unpublished observations, the side-chain properties of the aspartate residue seem to be critical for the generation of this signal, perhaps influencing local conformational dynamics that affect the T_2 relaxation rate and/or the proton exchange rate.

Some additional insights are provided by the fact that the midpoint potentials for the sq/hq couple displayed a more modest and opposite correlation with the free-energy difference between the type II and type II′ turns than that for the ox/sq couple (Figure 7). Because of the similar conformation of both reduced states, one might predict that contributions of $\Delta G_c^{sq/hq}$ and thus changes to this term as the result of the amino acid replacements should be very small. It is evident in Figure 6 that the increases in the binding free energy for the HQ states in response to the amino acid replacements were smaller than for the SQ. This phenomenon was observed previously for the Gly57 mutants and is interpreted as reflecting differing hydrogen-bonding strengths at N(5)H between the SQ and HQ states, i.e., differences in ΔG_i, with any modification in this interaction having a greater affect on the stability of the SQ (*13*). This is reasonable if you take into account the weaker N(5)H interaction in the fully reduced state due to the decrease in charge at this position when the flavin becomes more electron rich (*11*, *41*). Therefore, given the strong correlation between the midpoint potentials for *both* couples and the energy differences between the turn types and, within the assumptions and limitations of the computational studies, the similarity between the computed ΔΔG (II′ − II) values and the observed changes in the binding free energies principally for the OX and SQ states between which the conformational change occurs, we conclude that the amino acid replacements introduced at the two central positions of the *β*-turn primarily alter $\Delta G_c^{ox/sq}$ in Scheme 1, although the linkage of this effect to changes in ΔG_i cannot be entirely excluded.

Contributions of the cis Conformer. The central peptide bond in the reverse turn adopts three different conformations in the oxidized state of the *C. beijerinckii* flavodoxin; the trans O-up, the cis O-down, and trans O-down (*11*). These ambiguities complicate our analysis and this issue needs to be addressed more thoroughly. The conformational energies for the two turn types were calculated assuming a trans configuration of the peptide bond. However, to what extent would the cis configuration affect these values? More importantly, would the contributions of the cis conformer affect all the mutations equally and in so doing be factored out for this analysis?

Computational studies have predicted a change in the conformational energy of 1.8 kcal/mol for the cis-trans isomerization that occurs on going from the oxidized to the semiquinone state when a cis Gly-Asp (wild-type) sequence has been replaced by a cis Gly-Pro sequence (*11*). The

observed change of 1.4 kcal/mol for the Gly-Pro mutant being primarily due to differences in conformational energies would also reflect its altered conformer equilibrium, where wild-type consists of a mixture of cis O-down, trans O-down, and trans O-up species, the Gly-Pro mutant is all cis O-down. Yet the difference between the observed and predicted values differs by only 0.4 kcal/mol. (*11*). Also, a distribution of both the cis and trans O-down conformers is observed in the oxidized state (*11*). Both observations suggest that differences in cis and trans conformer equilibrium are not a major contributing factor as they may have relatively similar conformational energies.

A detailed analysis of these unusual Xaa-Xaa (where Xaa is any amino acid except proline) cis peptide bonds revealed a strong preference for the ϕ,ψ angles of the residues involved (*42*). All residues N-terminal and most residues C-terminal (except glycine) to a nonproline cis peptide bond are found in the β region of the Ramachandran plot. Presumably, any combination of residues is capable of adopting a cis peptide bond. Furthermore, it was observed that ψ_1 and ϕ_2 of the residues involved are restricted to only two energetically allowed conformations irrespective of ϕ_1 and ψ_2. The lack of significant structural differences on mutation of either of these residues in the *C. beijerinckii* flavodoxin is then not surprising (*11*). A later study calculated the preferences of amino acid residues to be involved in or adjacent to a cis peptide bond (*43*). The lack of bulky side chains on the two residues involved supported the inhibitory role these would have on the isomerization process. In keeping with this theory, small residues (glycine and alanine), which offer minimal steric resistance, should favor the cis form and, therefore, could be accommodated at both positions, as was observed. A strong preference for polar residues C-terminal to the cis peptide bond was also noted and it was believed that hydrogen bonding of these polar side chains with its main-chain amide would lower the activation energy and thus facilitates isomerization. Such a phenomenon may actually be occurring in wild-type flavodoxin, which has an aspartate residue C-terminal to the cis bond. But as this polar side chain has been uniformly removed in all mutants, such energetic contributions are not possible. This would strongly suggest that the contribution of the cis conformer would be similar for all these mutants. As the interpretations are based more on the comparison of the various mutants rather than the actual values, we believe that our analysis is valid.

Conclusions. For the first time, to our knowledge, this study more conclusively demonstrates a direct linkage between the conformational energetics of the protein induced by the sequence specificity of a β-turn and the modulation of the redox potentials of the flavin cofactor as previously postulated (*2*, *11*). This study also further illuminates the critical structural role of the often conserved glycine residue in the peptide loop adjacent to the N(5)/C(4)O edge of the flavin particularly in the thermodynamic stabilization of the neutral semiquinone state of the flavodoxin (*10*, *13*). These results could have more general implications regarding the role of protein conformational energetics/dynamics in the modulation of the activities of other proteins as well. For example, the interconversion of a β-turn in the HIV-1 protease occurs in a loop region upon inhibitor binding and is believed to facilitate function by allowing substrate access to and product release from the active site (*44*, *45*).

ACKNOWLEDGMENT

We acknowledge Dr. Lawrence Druhan whose insightful suggestions initiated this study and Dr. Charles E. Cottrell of the Campus Chemical Instrument Center for his assistance in obtaining the FT-NMR data. We also thank Dr. Martha L. Ludwig of the University of Michigan for the many valuable discussions on the structure of this flavodoxin and whose pioneering structural studies served to inspire this work.

REFERENCES

1. Mayhew, S. G., and Tollin, G. (1992) in *Chemistry and Biochemistry of Flavoenzymes* (Müller, F., Ed.) pp 389−426, CRC Press, Boca Raton, FL.
2. Ludwig, M. L., and Luschinsky, C. L. (1992) in *Chemistry and Biochemistry of Flavoenzymes* (Müller, F., Ed.) pp 427−466, CRC Press, Boca Raton, FL.
3. Swenson, R. P., and Krey, G. D. (1994) *Biochemistry 33*, 8505−14.
4. Zhou, Z., and Swenson, R. P. (1995) *Biochemistry 34*, 3183−92.
5. Chang, F. C., and Swenson, R. P. (1997) *Biochemistry 36*, 9013-21.
6. Hoover, D. M., Drennan, C. L., Metzger, A. L., Osborne, C., Weber, C. H., Pattridge, K. A., and Ludwig, M. L. (1999) *J. Mol. Biol. 294*, 725−43.
7. Zhou, Z., and Swenson, R. P. (1996) *Biochemistry 35*, 15980−8.
8. Lostao, A., Gomez-Moreno, C., Mayhew, S. G., and Sancho, J. (1997) *Biochemistry 36*, 14334−44.
9. Druhan, L. J., and Swenson, R. P. (1998) *Biochemistry 37*, 9668−78.
10. Bradley, L. H., and Swenson, R. P. (1999) *Biochemistry 38*, 12377−86.
11. Ludwig, M. L., Pattridge, K. A., Metzger, A. L., Dixon, M. M., Eren, M., Feng, Y., and Swenson, R. P. (1997) *Biochemistry 36*, 1259−80.
12. O'Farrell, P. A., Walsh, M. A., McCarthy, A. A., Higgins, T. M., Voordouw, G., and Mayhew, S. G. (1998) *Biochemistry 37*, 8405−16.
13. Chang, F. C., and Swenson, R. P. (1999) *Biochemistry 38*, 7168−76.
14. Burnett, R. M., Darling, G. D., Kendall, D. S., LeQuesne, M. E., Mayhew, S. G., Smith, W. W., and Ludwig, M. L. (1974) *J. Biol. Chem. 249*, 4383−92.
15. Smith, W. W., Burnett, R. M., Darling, G. D., and Ludwig, M. L. (1977) *J. Mol. Biol. 117*, 195−225.
16. Watenpaugh, K. D., Sieker, L. C., and Jensen, L. H. (1976) in *Flavins and flavoproteins: proceedings* (Singer, T. P., Ed.) pp 405−410, Elsevier Scientific, Amsterdam, New York.
17. Watt, W., Tulinsky, A., Swenson, R. P., and Watenpaugh, K. D. (1991) *J. Mol. Biol. 218*, 195−208.
18. Laudenbach, D. E., Straus, N. A., Pattridge, K. A., and Ludwig, M. L. (1988) in *Flavins and flavoproteins, 1987: proceedings of the Ninth International Symposium on Flavins and Flavoproteins* (Edmondson, D. E., and McCormick, D. B., Eds.) Atlanta, GA, June 7−12, 1987, pp 249−260, W. de Gruyter, Berlin.
19. Luschinsky, C. L., Dunham, W. R., Osborne, C., Pattridge, K. A., and Ludwig, M. L. (1991) in *Flavins and flavoproteins 1990: proceedings of the tenth international symposium* (Curti, B., Ronchi, S., and Zanetti, G., Eds.) Como, Italy, July 15−20, 1990, pp 409−413, W. de Gruyter, Berlin.
20. Drennan, C. L., Pattridge, K. A., Weber, C. H., Metzger, A. L., Hoover, D. M., and Ludwig, M. L. (1999) *J. Mol. Biol. 294*, 711−24.
21. Yan, Y., Erickson, B. E., and Tropsha, A. (1995) *J. Am. Chem. Soc. 117*, 7592−7599.
22. Yang, A. S., Hitz, B., and Honig, B. (1996) *J. Mol. Biol. 259*, 873−82.

23. Kunkel, T. A. (1985) *Proc. Natl. Acad. Sci. U.S.A. 82*, 488−92.
24. Clark, W. M. (1972) *Oxidation−reduction potentials of organic systems*, Robert E. Krieger Publishing Company, Huntington, NY.
25. Whitby, L. G. (1953) *Biochem. J. 54*, 437−442.
26. Wassink, J. H., and Mayhew, S. G. (1975) *Anal. Biochem. 68*, 609−16.
27. Anderson, R. F. (1983) *Biochim. Biophys. Acta 722*, 158−62.
28. Mayhew, S. G. (1999) *Eur. J. Biochem. 265*, 698−702.
29. Draper, R. D., and Ingraham, L. L. (1968) *Arch. Biochem. Biophys. 125*, 802−8.
30. Müller, F. (1991) *Chemistry and biochemistry of flavoenzymes*, Vol. 1, CRC Press, Boca Raton.
31. Ghisla, S., Massey, V., Lhoste, J. M., and Mayhew, S. G. (1974) *Biochemistry 13*, 589−97.
32. Yalloway, G. N., Mayhew, S. G., Malthouse, J. P., Gallagher, M. E., and Curley, G. P. (1999) *Biochemistry 38*, 3753−62.
33. Nakajima, N., Higo, J., Kidera, A., and Nakamura, H. (2000) *J. Mol. Biol. 296*, 197−216.
34. Dubourdieu, M., le Gall, J., and Favaudon, V. (1975) *Biochim. Biophys. Acta 376*, 519−32.
35. Witanowski, M., Stefaniak, L., and Webb, G. A. (1981) *Annu. Rep. NMR Spectrosc. 11B*, 1−493.
36. Vervoort, J., Muller, F., Mayhew, S. G., van den Berg, W. A., Moonen, C. T., and Bacher, A. (1986) *Biochemistry 25*, 6789−99.
37. Smith, J. A., and Pease, L. G. (1980) *CRC Crit. Rev. Biochem. 8*, 315−99.
38. Wilmot, C. M., and Thornton, J. M. (1988) *J. Mol. Biol. 203*, 221−32.
39. Richardson, J. S. (1981) *Adv. Protein Chem. 34*, 167−339.
40. Möhle, K., Gubmann, M., and Hofmann, H. (1997) *J. Comput. Chem. 18*, 1415−1430.
41. Hall, L. H., Orchard, B. J., and Tripathy, S. K. (1987) *Int. J. Quantum Chem. 31*, 217−242.
42. Jabs, A., Weiss, M. S., and Hilgenfeld, R. (1999) *J. Mol. Biol. 286*, 291−304.
43. Pal, D., and Chakrabarti, P. (1999) *J. Mol. Biol. 294*, 271−288.
44. Gunasekaran, K., Gomathi, L., Ramakrishnan, C., Chandrasekhar, J., and Balaram, P. (1998) *J. Mol. Biol. 284*, 1505−16.
45. Nicholson, L. K., Yamazaki, T., Torchia, D. A., Grzesiek, S., Bax, A., Stahl, S. J., Kaufman, J. D., Wingfield, P. T., Lam, P. Y., Jadhav, P. K., and et al. (1995) *Nat. Struct. Biol. 2*, 274−80.

BI001519A